

Electron Transport Mechanism in GaN/AlGaN HEMT Structures

Sibel GÖKDEN

*Balikesir University, Department of Physics, Balikesir-TURKEY
e-mail: sozalp@balikesir.edu.tr*

Received 02.12.2002

Abstract

The electron transport mechanism in GaN/AlGaN HEMT (High Electron Mobility Transistors) structures grown with MBE on sapphire substrate was investigated by using the temperature dependence of the Hall coefficient, resistivity, carrier density and Hall mobility. Hall measurements were carried out using Van der Pauw geometry. From the LO-phonon-scattering-limited component of the mobility, we obtain LO phonon energy $\hbar\omega \approx 90$ meV and the momentum relaxation time of $\tau_m \approx 4$ fs. Also, from the temperature dependence of the 2D carrier density, we obtain the donor activation energy $E_a \approx 29$ meV.

Key Words: GaN, Momentum Relaxation, LO Phonon Scattering.

1. Introduction

Gallium nitride (GaN), a III-V semiconductor, has increasingly become of interest for use in many semiconductor device structures. Due to its very large band gap (3–4 eV), GaN offers some important advantages in various applications. In particular GaN is a candidate for high power, high temperature, and high-frequency electronic applications. In order to utilize GaN to its fullest potential in these applications, a good understanding of the transport properties of the charge carriers in GaN is essential. The most important and widely material transport parameters are the temperature dependence of the mobility and the field dependence of the carrier drift velocity [1].

In this paper, we report the temperature dependence of the Hall coefficient, resistivity, 2D carrier density and Hall mobility. Then, we compare the obtained LO phonon energy $\hbar\omega \approx 90$ meV, momentum relaxation time $\tau_m \approx 4$ fs and the donor activation energy $E_a \approx 29$ meV with existing observations.

2. Experimental Technique

The sample investigated in this work was grown using MBE on tungsten-backed sapphire substrates. Tungsten is evaporated onto the sapphire to act as a heat sink to dissipate excess thermal energy at high electric fields. The thickness of the GaN buffer layer is 3 μm , and the Al concentration of the 250 Å thick GaAlN layer is 30% as determined from PL measurements. The Van der Pauw geometry was used for performing Hall and resistivity measurements. A sample with Van der Pauw type geometry is shown in Figure 1. The sample is square-shaped and has four ohmic contact in the corners. Indium was annealed onto both samples to provide ohmic contacts. The contacts must be at the very edges of the sample and much smaller than the sample area. In the Van der Pauw measurements, a constant current of 1 μA was applied between two of the four contacts, e.g. the current enters through contact A and leaves through contact B, and a magnetic field between 0.35 T and 3 T was applied perpendicular to the sample surface. Then, the

voltage between the contact C and D was measured. The measurement was done at lattice temperatures between 4.2 and 300 K.

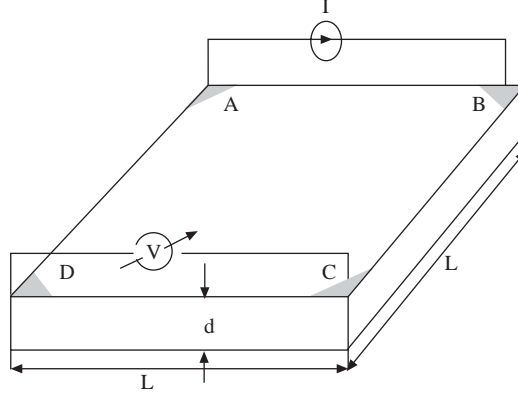


Figure 1. Van der Pauw Geometry used for Hall measurements.

If by $R_{AB,CD}$ one denotes the ratio of the voltage V_{CD} between contacts C and D, to the current I_{AB} flowing between A and B, then Van der Pauw has shown that [2]

$$\exp\left(-\frac{\pi d}{\rho}R_{AB,CD}\right) + \exp\left(-\frac{\pi d}{\rho}R_{BC,AD}\right) = 1 \quad (1)$$

If the contacted wafer is completely symmetrical as in Figure1, resistivity are given by

$$\rho = \frac{\pi d}{\ln 2} \frac{V_{CD}}{I_{AB}}, \quad (2)$$

where d is the thickness of the sample.

Also, the relations for the sheet carrier concentration and Hall mobility for the Van der Pauw geometry are written by [2]

$$n = \frac{BI_{AB}}{eV_{CD}} \quad (3)$$

and

$$\mu_H = \frac{d}{B\rho} \Delta R_{AB,CD}, \quad (4)$$

where B is the magnetic field applied perpendicular to the sample surface, $\Delta R_{AB,CD}$ is the compared value to $R_{AB,CD}$'s zero magnetic field value.

From Eq. (3), the Hall coefficient can be written as

$$R_H = \frac{1}{ne}$$

or

$$R_H = \mu\rho. \quad (5)$$

3. Experimental Results

Figure 2 shows the temperature dependence of the Hall coefficient. For the GaN/AlGaN HEMT structure, at $T_L = 4.2$ K the Hall coefficient is $R_H = 4.13 \times 10^{-5} \text{ m}^2/\text{V}\cdot\text{s}$. It decreases very little with temperature up to $T_L = 80$ K, then decreases rapidly down to $R_H = 3.06 \times 10^{-5} \text{ m}^2/\text{V}\cdot\text{s}$ at $T_L = 300$ K. The resistivity versus T_L is shown Figure 3. Also, at $T_L = 4.2$ K the resistivity is $\rho = 1.46 \times 10^{-4} \text{ ohm}\cdot\text{m}$. It increases very little with temperature up to $T_L = 80$ K, then increases rapidly up to $\rho = 4.08 \times 10^{-4} \text{ ohm}\cdot\text{m}$ at $T_L = 300$ K.

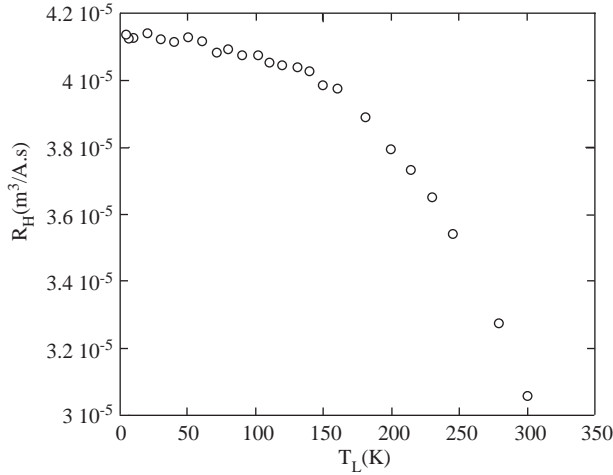


Figure 2. Hall coefficient versus lattice temperature.

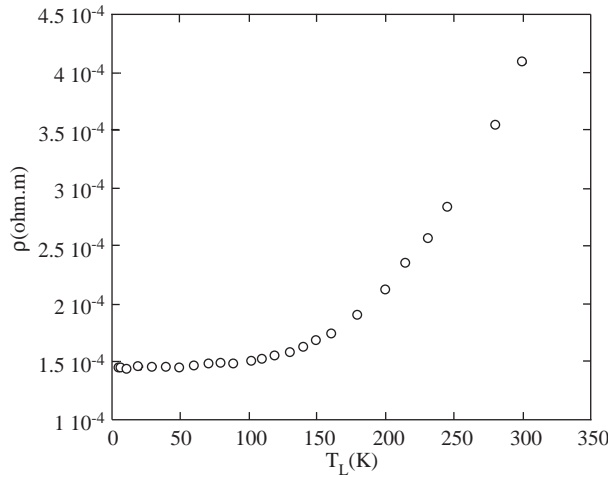


Figure 3. Resistivity versus lattice temperature.

Figure 4 shows the two-dimensional carrier density and Hall mobility between lattice temperature $T_L = 4.2$ K and 300 K, respectively. The two-dimensional electron density at $T_L = 4.2$ K is $n = 1.5 \times 10^{13} \text{ cm}^{-2}$. It remains constant up to $T_L = 150$ K, then increases rapidly to $n = 2.1 \times 10^{13} \text{ cm}^{-2}$ at $T_L = 300$ K. The high density of electrons is due to large spontaneous and strain-induced polarization in the GaN/AlGaN interface as commonly predicted and observed [3]. The increase in the carrier density at high temperature is due to parallel conduction in the AlGaN layer. At 4.2 K the Hall mobility is $\mu = 2830 \text{ cm}^2/\text{V}\cdot\text{s}$. It decreases very little (by 3%) with temperature up to $T_L = 80$ K, then decreases rapidly down to $\mu = 743 \text{ cm}^2/\text{V}\cdot\text{s}$ at $T_L = 300$ K. Due to the finite parallel conductivity in the GaN layer according to [4] at high temperatures, the measured Hall carrier density and Hall mobility are given as

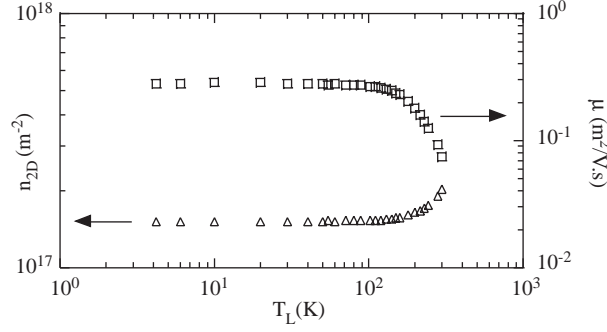


Figure 4. Two-dimensional electron density and Hall mobility versus lattice temperature.

$$n_H = \frac{n_1\mu_1 + n_2\mu_2}{\mu_H} \quad (6)$$

$$\mu_H = \frac{n_1\mu_1^2 + n_2\mu_2^2}{n_1\mu_1 + n_2\mu_2} \quad (7)$$

where n_H and μ_H are the measured Hall carrier density and Hall mobility and n_1 , n_2 , μ_1 and μ_2 are the two-dimensional carrier density in GaN, sheet density in AlGaIn and electron mobilities in GaN and AlGaIn, respectively [1].

In Figure 5, the inverse of optic phonon limited electron mobility versus inverse lattice temperature is plotted between $T_L = 4.2$ K and 300 K. In GaN/AlGaIn HEMT structures, interface roughness scattering saturates the mobility at low temperatures ($T_L < 180$ K). At high temperatures ($T_L > 180$ K), however, mobility decreases gradually with increasing temperature. In order to obtain the dominant scattering mechanism that limits the mobility at high temperatures, we used Matthiessen's rule. In the high temperature region of Figure 4 ($T_L > 180$ K), there is an exponential dependence as would be expected from a scattering mechanism involving LO phonons, in the form [5]

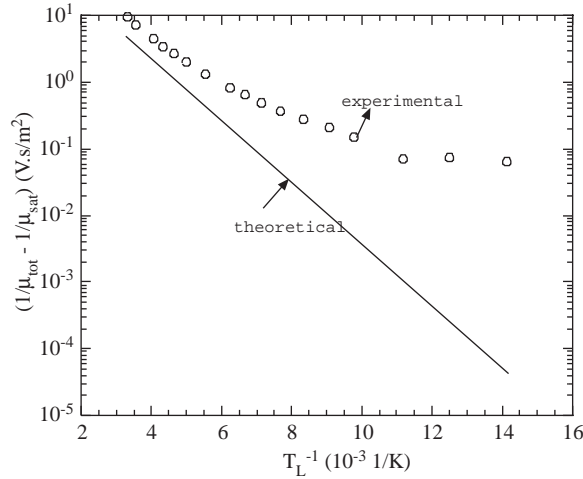


Figure 5. The inverse of the LO-phonon-limited electron mobility versus inverse lattice temperature [1]. Open circles: experimental results, obtained from the measured Hall mobility versus temperature data using Matthiessen's rule. Line: theoretical calculation using Equation (6).

$$\frac{1}{\mu_{LO}} = \frac{m^*}{e\tau_m} \exp\left(-\frac{\hbar\omega}{kT_L}\right), \quad (8)$$

where $m^* = 0.22 m_0$, In the plot we took momentum relaxation time, τ_m as the electron phonon scattering time constant, $\tau_0 = 8 \times 10^{-15} s$. We can, therefore, use Matthiesen's rule to separate the LO phonon scattering limited component of the mobility via

$$\frac{1}{\mu_{LO}} = \frac{1}{\mu_t} + \frac{1}{\mu_0}, \quad (9)$$

where μ_0 is the low temperature mobility and μ_t is the measured temperature dependent mobility. A plot of the logarithm of $1/\mu_{LO}$ determined from the experimental results plotted against $1/T_L$ as in Eq. 8 was used to extract $\hbar\omega$ and τ_m . We obtain $\hbar\omega = 90$ meV. This is in good agreement with the theoretical value [6]. However, at 300 K the magnitude of the experimental data is about a factor of two higher than that in Eq. (8). This suggests a momentum relaxation time of $\tau_m = \tau_0/2 = 4 \times 10^{-5} s$, a value much smaller than the theoretically expected electron momentum relaxation time [7-9] but in accord with other observations [10-12]. The reason for the reduced momentum relaxation time and hence mobility compared with the theory is not clear to us. Interface roughness scattering is often invoked as a cause of reduced mobility in GaN/AlGaIn [5].

Also, Figure 6 shows the log of 2D carrier density versus inverse lattice temperature. The dependence of the carrier density on temperature with a donor activation energy E_a is given by [13]

$$n_{2D} \propto \exp\left(-\frac{E_a}{2k_B T_L}\right), \quad (10)$$

where k_B is Boltzman's constant. From Equation (10), we obtain $E_a \approx 29$ meV. This is in agreement with other observations [14, 15].

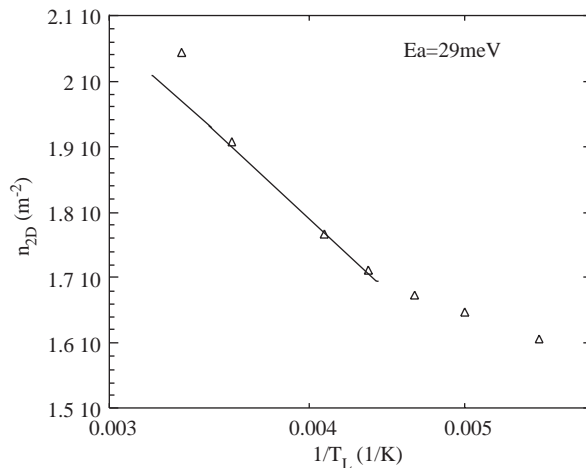


Figure 6. 2D carrier density versus inverse lattice temperature. The solid line: theoretical calculation using Equation (8).

4. Conclusion

We have studied the transport mechanism of two-dimensional electron gas, which is formed at a GaN/AlGaIn interface as a result of spontaneous and piezoelectric polarization, in the e-LO phonon scattering regime. We obtain the LO phonon energy, momentum relaxation time and the donor activation energy are $\hbar\omega \approx 90$ meV, $\tau_m \approx 4$ fs, $E_a \approx 29$ meV, respectively.

Acknowledgments

I am grateful to Prof. Dr. Naci Balkan and Prof. Dr. M. Çetin Arıkan for supporting this work.

References

- [1] N. Balkan, M.C. Arikan, S. Gokden, V. Tilak, B. Schaff and R.J. Shealy, *J. Phys.: Condensed Matter*, **14**, (2002), 3457.
- [2] Philips, *Technical Review*, **20**, (1958/59), 220-224.
- [3] B.K. Ridley, *Appl. Phys. Lett.*, **77**, (2000), 990.
- [4] M.J. Kane, D.A. Anderson, L.L. Taylor and T. Kerr, *J. Phys. C: Solide State Phys.*, **18**, (1985), 5629.
- [5] B.K. Ridley, B.E. Foutz, L.F. Eastman, *Phys. Rev. B*, 61, **24**, (2000),16862.
- [6] N.M. Stanton, A.J. Kent, A.V. Akimov, P. Hawker, T.S. Cheng, C. T. Foxon, *J. Appl. Phys.*, **89(2)**, (2001), 973.
- [7] S.T. Sheppard, K. Doverspike, W.L. Pribble, S.T. Allen, J.W. Palmour, L.T. Kehias and T. J. Jenkins, *IEEE Trans. Electron Devices*, **20**, (1999), 161.
- [8] J.J. Harris et al., *Semicond. Sci. Technol.*, **16**, (2001), 402.
- [9] B.K. Ridley, *J. Appl. Phys.*, **84**, (1998), 4020.
- [10] X.Z. Dang, P.M. Asbeck, E.T. Yu, G.J. Sullivan, M.Y. Chen, B. T. Mc Dermptt, K.S. Boutros and, J.M. Redwing, *Appl. Phys. Lett.*, **74**, (1999), 3890.
- [11] R. Gaska, M.S. Shur, A.D. Bykovski, A.O. Orlov and G.L. Snider, *Appl. Phys. Lett.*, **74**, (1999), 287.
- [12] R. Oberhuber, G. Zandler and P. Vogl, *Appl. Phys. Lett.*, **73**, (1998), 1243.
- [13] S.M. Sze, *Physics of Semiconductor Decices*, ed. 2nd, (Wiley, NewYork,1981), p.245.
- [14] R.J. Molnar, T. Lei, and T.D. Moustakas, *Appl. Phys. Lett.*, **62**, (1992), 72.
- [15] D. Doppalapudi, and T.D. Moustakas, *J. Appl. Phys.*, **73**, (1998), 821.